Correlated and Uncorrelated Debye–Waller Factors and Correlation Function in Atomic Vibrations Including Many-Body Effects

N. Van Hung* and N. Cong Toan

Department of Physics, VNU University of Science, 334 Nguyen Trai, Thanh Xuan, Hanoi, Vietnam

Received: 10.02.2024 & Accepted: 09.05.2024

Doi: 10.12693/APhysPolA.146.95 *e-mail: hungnv@vnu.edu.vn

Correlated and uncorrelated Debye–Waller factors and correlation function in atomic vibrations described by mean square relative displacement, mean square displacement, and displacement–displacement correlation function, respectively, have been studied based on correlated and uncorrelated Einstein models, including many-body effects. The impact of many-body effects in the derived analytical expressions of the above-considered quantities is realized by using the effective potentials of the derived Einstein models, which take into account the contributions of all nearest neighbors of vibrating atoms. The Morse potential is used to describe the single-pair atomic interactions. The difference between the correlated Debye–Waller factor and the uncorrelated one is considered to be the source of the correlation effect described by the correlation function, which is temperature- and crystal-type-dependent. The larger such difference is, the stronger the correlation effect it generates. The numerical results for the Cu crystal agree with experimental results and with those calculated using other theories.

topics: correlated and uncorrelated Debye–Waller factors, correlation function, correlated and uncorrelated Einstein models, effective potentials and many-body effects

1. Introduction

Thermal atomic vibrations and disorders in extended X-ray absorption fine structure (EXAFS) spectroscopy and other related spectroscopy give rise to Debye–Waller factors (DWFs) [1–26]. These factors used in EXAFS and related spectra depend on the temperature T as $e^{-W(T)}$ and on the wave number k (or energy). For EXAFS spectroscopy, $W(T) \approx 2k^2\sigma^2(T)$, where $\sigma^2(T)$ is the mean square relative displacement (MSRD) of bond between absorber and backscatter atoms. The EXAFS DWF is analogous to factor found in X-ray and neutron diffraction or the Mössbauer effect, where $W(T) = \frac{1}{2}k^2u^2(T)$. The difference is that the EXAFS DWF refers to correlated averages over relative displacements, as is the case of the MSRD $\sigma^2(T)$, while in X-ray absorption or neutron diffraction, $u^2(T)$ refers to the mean square displacement (MSD) of a given atom. Unfortunately, the MSRD or correlated DWF $\sigma^2(T)$ and the MSD or uncorrelated DWF $u^2(T)$ are closely related with one another and from them, the displacement–displacement correlation function (DCF) or correlation function $C_R(T)$ describing the correlation effects is generated. Accurate DWFs and other related functions such as $u^2(T)$ and $C_R(T)$ are crucial to quantitative treatment of the X-ray absorption spectra and different effects in EXAFS theory.

Many efforts have been made to derive procedures for studying DWFs of materials. Satisfactory procedures are those of classical methods [2–6], which have the advantages of simplicity and work very well at high temperatures, except for limitations at low temperatures due to the absence of zero-point vibration. Importantly, the derived procedures include also quantum methods, which have the advantages of working at both low and high temperatures. These include, for example, the effective anharmonic single-particle potential method [7], the single bond correlated Einstein model [8], the path integral effective potential [9], the full lattice dynamical (FLD) approach [10, 11], the local force constant theory [12], the dynamic matrix calculation [13], the path-integral Monte Carlo calculation [14], the anharmonic correlated Einstein model (ACEM) [15], the anharmonic correlated Debye model [16], and many others. The efforts undertaken have proven to make significant contributions to materials research, for example [17–24]. Here, ACEM is successfully applied in the development of several methods such as: EXAFS theory including anharmonic contributions [17], method for studying EXAFS of doping

materials compared to Mössbauer studies [18], pressure effects in EXAFS [19], thermodynamic properties of isotopes [20] and of semiconductors [21]. Moreover, based on DWFs, the effective methods have been derived for studying strong anharmonicity in tin monosulfide evidenced by local distortion, high-energy optic phonons [22], melting curve, eutectic point, Lindemann's melting temperature of close-packed hexagonal (hcp) binary alloys [23], and a semi-classical ACEM for hcp crystals [24]. Unfortunately, there are still few works [25, 26] concerning the uncorrelated DWF $u^2(T)$ and the DCF or correlation function $C_R(T)$ describing the correlation effects in atomic vibrations.

The purpose of this work is to derive the method enabling the calculation and analysis of correlated and uncorrelated DWFs and then correlation function in atomic vibrations (i.e., σ^2, u^2, and C_R, described, respectively, by MSRD, MSD, and DCF), including many-body effects. In Sect. 2 the analytical expressions have been derived for the correlated DWF $\sigma^2(T)$ based on the correlated Einstein model (CEM) using a correlated atomic vibration (CAV) and for the uncorrelated DWF $u^2(T)$ based on the uncorrelated Einstein model (UCEM) using a single atomic vibration (SAV). The correlation function $C_R(T)$ is generated from the difference between the derived $\sigma^2(T)$ and $u^2(T)$. The many-body effects given in the derived analytical expressions of $\sigma^2(T)$, $u^2(T)$ and $C_R(T)$ are obtained based on the CEM and UCEM effective potentials, which include contributions of all nearest neighbors of the absorber and backscatter atoms in the case of CEM and of a single atom in the case of UCEM. The created method leads to the simplification of the operation of a many-body system in the EXAFS theory to a useful one, which is a one-dimensional model. The Morse potential is assumed to describe the single-pair atomic interactions. The numerical results for Cu (Sect. 3), i.e., for one of the intensively studied crystals, are compared with: (i) experimental values taken from the measured Morse parameters (MMP) [27], (ii) measured values [7, 27–29] for $\sigma^2(T)$, and also (iii) with values calculated using other theories [25, 26] for the ratio C_R/u^2, which in fact show good agreement. Conclusions on the obtained results are presented in Sect. 4.

2. Correlated and uncorrelated DWFs and correlation function based on CEM and UCEM

2.1. Relation of correlation function with correlated and uncorrelated DWFs

The definition of MSRD or correlated DWF $\sigma^2(T)$ implies its close relation with the MSD or uncorrelated DWF u^2(T) and the DCF or correlation function C_R(T). It can be written as

$$\sigma^2(T) = \left\langle \left[\hat{\boldsymbol{R}}^0 \cdot (\boldsymbol{u}_i - \boldsymbol{u}_0)\right]^2 \right\rangle = 2u^2(T) - C_R(T), \tag{1}$$

where $\boldsymbol{u}_i - \boldsymbol{u}_0$ included in the first equation of (1) contains the atomic displacements of the i-th and 0-th sites defined by their displacements from those of the equilibrium positions, $\hat{\boldsymbol{R}}^0$ is the unit vector pointing from the 0-th site towards the i-th site, and the bracket $\langle \ldots \rangle$ denotes the thermal average.

Moreover, in the second equation of (1), the uncorrelated DWF or MSD u^2(T) has been defined as

$$u^2(T) = \left\langle \left(\boldsymbol{u}_0 \cdot \hat{\boldsymbol{R}}^0\right)^2 \right\rangle = \left\langle \left(\boldsymbol{u}_i \cdot \hat{\boldsymbol{R}}^0\right)^2 \right\rangle, \tag{2}$$

and then the DCF of correlation function C_R(T) had to take the form

$$C_R(T) = 2\left\langle \left(\boldsymbol{u}_0 \cdot \hat{\boldsymbol{R}}^0\right)\left(\boldsymbol{u}_i \cdot \hat{\boldsymbol{R}}^0\right) \right\rangle = 2u^2(T) - \sigma^2(T), \tag{3}$$

which is apparently obtained by the difference between the correlated and uncorrelated DWFs.

2.2. Effective potentials of CEM and UCEM

In order to specify the thermodynamic parameters, it is necessary to determine the local force constants [7–21]. The effective potential applied in the present theory can be expressed as a function of the displacement $x = r - r_0$ along the direction $\hat{\boldsymbol{R}}^0$, with r and r_0 being the instantaneous and equilibrium distances between the absorber and backscatter atoms. Thus, the expressions of the potencial for the CEM using CAV ($V_{\rm eff}^C(x)$) and for the UCEM using SAV ($V_{\rm eff}^S(x)$) have the following forms

$$V_{\rm eff}^{C(S)}(x) \approx \frac{1}{2} k_{\rm eff}^{C(S)} x^2, \tag{4}$$

where the difference of the mentioned potentials is caused by the difference between their effective local force constants $k_{\rm eff}^C$ for the CAV model and $k_{\rm eff}^S$ for the SAV model, used in the present theory.

Note that since atomic correlations do not involve anharmonic contribution, the effective interatomic interaction potential given by (4) only includes harmonic terms.

The values of $k_{\rm eff}^C$ for the atomic correlated effective potential can be obtained by comparing the potential $V_{\rm eff}^C(x)$ of (4) to that defined for a single bond pair in the center-of-mass frame [14] of the absorber with mass M_1 and the backscatter atoms with mass M_2. Therefore, we have

$$V_{\rm eff}^C(x) = V(x) + \sum_{j \neq i} V\left(\frac{\mu}{M_i} x\, \hat{\boldsymbol{R}}_{12} \cdot \hat{\boldsymbol{R}}_{ij}\right) = V(x) + 2V\left(-\frac{x}{2}\right) + 8V\left(-\frac{x}{4}\right) + 8V\left(\frac{x}{4}\right), \tag{5}$$

where the first term on the right concerns only absorber and backscatter atoms, the second one,

containing the sum i over absorber ($i = 1$) and backscatter ($i = 2$) and the sum j over their remaining nearest neighbors, describes the lattice contributions or many-body effect to the pair interaction and depends on crystal structure type. Here, $\hat{\boldsymbol{R}}$ is the bond unit vector. The second equation of (5) is for the monatomic face-centered cubic (fcc) crystals, in which the reduced mass $\mu = M_1M_2/(M_1 + M_2)$ is replaced by $M/2$ because $M = M_1 = M_2$ stands for the atomic mass.

The values of $k^S_{\rm eff}$ are obtained by using the potential $V^S_{\rm eff}(x)$ of (4) and a method [30] for the single-atom effective potential, which takes into account only the influence of N nearest atomic neighbors of the central atom as

$$V^S_{\rm eff}(x) = \sum_{j=1}^{N} V\left(x\hat{\boldsymbol{R}}^0 \cdot \hat{\boldsymbol{R}}_j\right) = V(x) + V(-x) + 4V\left(\frac{x}{2}\right) + 4V\left(-\frac{x}{2}\right), \tag{6}$$

where $\hat{\boldsymbol{R}}_j$ are the unit vectors of the nearest neighboring atoms with respect to the equilibrium position of the central atom. The second equation of (6) is for monatomic fcc crystals.

The advantage of applying the effective potentials given by (5) for CEM and (6) for UCEM in the present theory is the possibility of taking into account many-body effects or lattice contributions. This is achieved by including the contributions of all nearest neighbors of the absorber and backscatter atoms for the CEM and of a single atom for the UCEM, where these derived effective potentials are presented as one-dimensional. In this manner, a complicated task of many-body system in EXAFS theory is simplified to one-dimensional model.

To describe a single-pair atomic interaction, we use the Morse potential expanded up to second order (harmonic term) around its minimum

$$V(x) = D\left(\mathrm{e}^{-2\alpha x} - 2\mathrm{e}^{-\alpha x}\right) \approx D\left(-1 + \alpha^2 x^2\right), \tag{7}$$

where α describes the width of the potential, and D is the dissociation energy.

Based on the atomic structure of the fcc crystal, the effective local force constants $k^C_{\rm eff}$ of CEM and $k^S_{\rm eff}$ of UCEM, given indirectly by the Morse potential parameters in (4), could be written here as

$$k^C_{\rm eff} = 5D\alpha^2, \qquad k^S_{\rm eff} = 8D\alpha^2. \tag{8}$$

Note that the significant difference between the above $k^S_{\rm eff}$ and $k^C_{\rm eff}$ will lead to a difference of the EXAFS quantities obtained from CEM and UCEM.

2.3. Analytical expressions of correlated and uncorrelated DWFs as well as correlation function

Based on CEM, the analytical expression of the temperature-dependent correlated DWF or MSRD $\sigma^2(T)$ using CAV has been derived and given by

$$\sigma^2(T) \cong \langle x^2 \rangle = \sigma_0^2 \frac{1+z}{1-z}, \qquad \sigma_0^2 = \frac{\hbar\omega^C_E}{k^C_{\rm eff}}, \tag{9}$$

$$z = \exp\left(-\frac{\theta^C_E}{T}\right), \qquad \theta^C_E = \frac{\hbar\omega^C_E}{k_{\rm B}}, \qquad \omega^C_E = \sqrt{\frac{k^C_{\rm eff}}{\mu}}, \tag{10}$$

where μ is the reduced mass of correlated vibrating atoms and $k_{\rm B}$ is the Boltzmann constant.

Similarly, based on UCEM, the analytical expression of the temperature-dependent uncorrelated DWF or MSD u^2(T) using SAV has been derived and given in the form

$$u^2(T) = u_0^2 \frac{1+z_1}{1-z_1}, \qquad u_0^2 = \frac{\hbar\omega^S_E}{k^S_{\rm eff}}, \tag{11}$$

$$z_1 = \exp\left(\frac{-\theta^S_E}{T}\right), \qquad \theta^S_E = \frac{\hbar\omega^S_E}{k_{\rm B}}, \qquad \omega^S_E = \sqrt{\frac{k^S_{\rm eff}}{M}}, \tag{12}$$

where M is the mass of a composite atom.

In the above analytical expressions, the CEM frequencies and temperatures are given by, respectively,

$$\omega^C_E = \sqrt{\frac{k^C_{\rm eff}}{\mu}} \qquad \text{and} \qquad \theta^C_E = \frac{\hbar\omega^C_E}{k_{\rm B}}, \tag{13}$$

and the UCEM frequencies and temperatures are given by, respectively,

$$\omega^S_E = \sqrt{\frac{k^S_{\rm eff}}{M}} \qquad \text{and} \qquad \theta^S_E = \frac{\hbar\omega^S_E}{k_{\rm B}}. \tag{14}$$

Consequently, the correlation function $C_R(T)$ describing the correlation effect is calculated using (3) based on the above expressions for the uncorrelated DWF $u^2(T)$ and correlated DWF $\sigma^2(T)$. The derived correlation function has the form

$$C_R(T) = 2u_0^2 \frac{1+z_1}{1-z_1} - \sigma_0^2 \frac{1+z}{1-z}, \tag{15}$$

where σ_0^2, z and u_0^2, z_1 are defined in (9)–(10) and (11)–(12), respectively.

Hence, the correlation function $C_R(T)$ describing the correlation effects of atomic vibrations in the materials results from the difference between the correlated DWF $\sigma^2(T)$ and the uncorrelated DWF $u^2(T)$. It has the same unit as DWF, behaving as a thermodynamic parameter. Actually, the reason causing this correlation effect can be attributed to the difference between the local force constants $k^C_{\rm eff}$ and $k^S_{\rm eff}$, as well as the difference between the reduced mass μ in CEM using CAV and the mass M of a composite atom in UCEM using SAV. This property will be discussed in detail through the numerical results presented in Sect. 3 for Cu as a fcc crystal.

Note that the functions $\sigma^2(T)$, u^2(T), and C_R(T) obtained above include many-body effects or lattice contributions because they contain the effective local force constants $k^C_{\rm eff}$ and $k^S_{\rm eff}$ describing the correlated and uncorrelated DWFs which actually include many-body effects.

3. Numerical results and discussions

Now, the expressions derived in the previous sections are applied to the numerical calculations for Cu in the fcc phase. Using the Morse potential parameters of Cu [31], i.e., $D = 0.3429$ eV, $\alpha = 1.3588$ Å^{-1}, and its measured Morse parameters, i.e., (MMP) [27] $D = 0.33$ eV, $\alpha = 1.38$ Å^{-1}, the effective local force constants $k^C_{\rm eff}$, $k^S_{\rm eff}$, as well as the correlated Einstein frequencies ω^C_E and temperature θ^C_E, and the uncorrelated Einstein frequency ω^S_E and temperature θ^S_E with respect to CAV in CEM and to SAV in UCEM, respectively, have been calculated. Some of the results are included in Table I.

The calculated results for the above-considered quantities of Cu written in Table I show the significant differences between the CAV model (with upper index "C") and the SAV model (with upper index "S"). The effective local force constant for the SAV model ($k^S_{\rm eff}$) is much larger than the one ($k^C_{\rm eff}$) for the CAV model. The reasons for this difference can be attributed to the difference in the number and mass of vibrating particles, because in the CAV model, there is only half of them compared to the SAV model. Actually, in the center-of-mass frame of single bond pair for the CAV model, the crystal behaves as it consists of quasi-atoms having a reduced mass that equals only half the composite mass of the atom, as shown in (5), and their number is only half the atomic number for the SAV model, because each quasi-atom is constructed from a pair of composite atoms. This difference also leads to the result, in which the values of correlated Einstein frequency ω^C_E and temperature θ^C_E obtained from the CAV model are larger than, respectively, ω^S_E and θ^S_E, obtained from the SAV model (Table I). Here, the value of $\theta^C_E = 234$ K calculated using the present theory (Table I) is close to the experimental result of 232 K [3, 29].

Figure 1 illustrates the effective potentials $V^{C(S)}_{\rm eff}(x)$ of Cu calculated using the present theory for the CAV and SAV models, which agree well with the experimental values (Exper.) obtained from MMPs [27]. Here, the SAV potential $V^S_{\rm eff}(x)$ is bigger than the CAV potential $V^C_{\rm eff}(x)$ because the effective local force constant for the SAV model ($k^S_{\rm eff}$) is larger than the one ($k^C_{\rm eff}$) for the CAV model (Table I). This means that the atomic interaction described by the SAV model or the CEM is stronger than the one for the CAV model or the UCEM. This discrepancy also leads to the difference between other quantities such as ω^C_E, θ^C_E (calculated using CEM) and ω^S_E, θ^S_E (calculated using UCEM), written in Table I. Such properties can be understood because the number and the mass of atoms in the SAV model are larger than those of the quasi-atoms in the CAV model.

Figure 2 illustrates the temperature dependence of the Debye–Waller factors: correlated DWF or MSRD $\sigma^2(T)$, uncorrelated DWF or MSD $u^2(T)$,

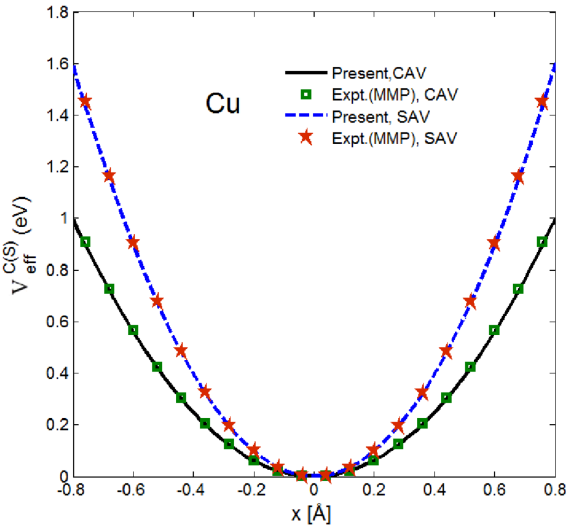

Fig. 1. Effective potentials $V^{C(S)}_{\rm eff}(x)$ of Cu, calculated using the present theory for CAV in CEM and for SAV in UCEM, and compared to the experimental values (Exper.) [27].

TABLE I

The values of $k^C_{\rm eff}$, $k^S_{\rm eff}$, ω^C_E, θ^C_E, ω^S_E, θ^S_E for Cu, calculated using the present theory and compared to the experimental values (Exper.) obtained from the MMPs [26].

Quantities	Present	Exper. [26]
$k^C_{\rm eff}$ [N/m]	49.7867	50.3450
$k^S_{\rm eff}$ [N/m]	79.6587	80.5520
ω^C_E ($\times 10^{13}$) [Hz]	3.0628	3.0799
ω^S_E ($\times 10^{13}$) [Hz]	2.7394	2.7547
θ^C_E [K]	233.9531	235.2611
θ^S_E [K]	209.2540	210.4239

and correlation function DCF $C_R(T)$ obtained from the difference, and also $\sigma^2(T)$ and $u^2(T)$ of Cu calculated using the present theory. They are all linear with T at high temperatures, beginning from the Einstein temperature where the classical limit applies, and they contain zero-point energy contributions at low temperatures, which is a quantum effect. Here, the calculated results of $\sigma^2(T)$, $u^2(T)$, $C_R(T)$ agree well with experimental values (Exper.) obtained from MMPs [26] and with the measured values for $\sigma^2(T)$, labeled as Exper. (1) [28], Exper. (2) [29], Exper. (3) [27], Exper. (4) [7]. Moreover, the values of $\sigma^2(T)$ are greater than those of $u^2(T)$, and that makes the damping factor in the EXAFS and other related spectroscopy for the SAV model greater than for the CAV model.

Note that the difference between the obtained correlated DWF $\sigma^2(T)$ and the uncorrelated one $u^2(T)$ of Cu, shown in Fig. 2, is the source causing the correlation effect described by $C_R(T)$. Hence,

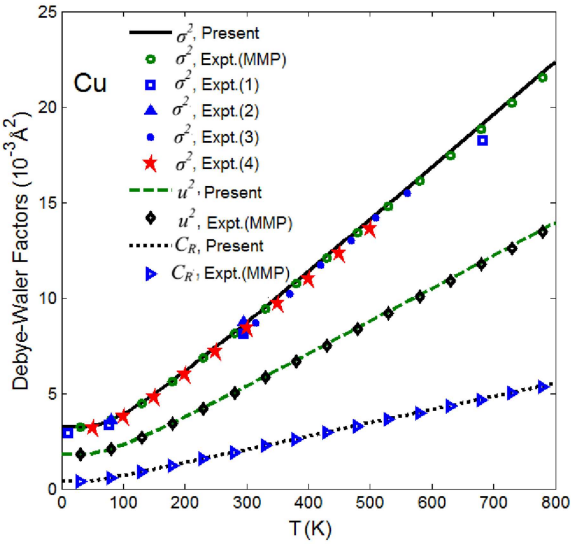

Fig. 2. Temperature dependence of correlated DWF $\sigma^2(T)$, uncorrelated DWF $u^2(T)$,and correlation function $C_R(T)$ of Cu, calculated using the present theory. The results are compared to the experimental values (Exper. (MMP)) obtained from MMPs [26] and the measured values for $\sigma^2(T)$: Exper. (1) [28], Exper. (2) [29], Exper. (3) [27], Exper. (4) [7], at different temperatures.

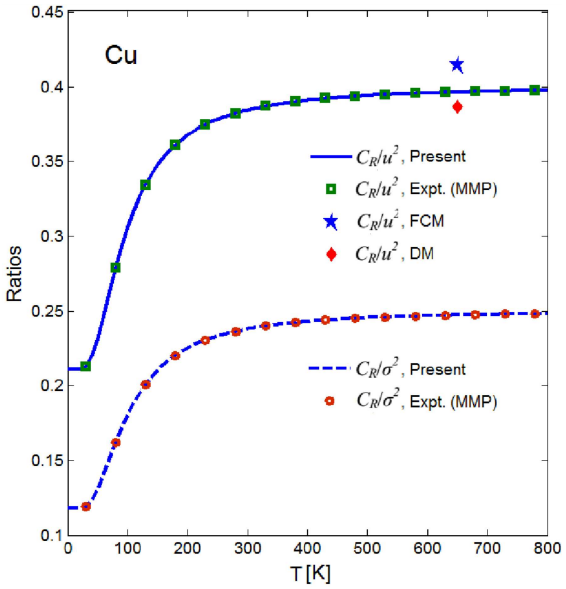

Fig. 3. Temperature dependence of the ratios C_R/u^2 and C_R/σ^2 of Cu, calculated using the present theory. The results are compared to experimental values (Exper. (MMP)) obtained from MMPs [27], as well as to the results calculated using the force constant model (FCM) [25] and Debye model (DM) [26] for the ratio C_R/u^2.

the correlation effect of Cu clearly depends on this difference appearing in different crystals. Figure 2 also shows that the larger difference between $\sigma^2(T)$ and $u^2(T)$ generates stronger correlation effect than the lesser one. Here, the correlation function $C_R(T)$ (Fig. 2) at high temperatures is stronger than at low temperatures. Moreover, the correlation effect has resulted only from the effective local force constants of the harmonic interatomic interaction potential, which clearly proves that it is a harmonic effect.

The ratio C_R/u^2 is often considered in studying EXAFS correlation effects [25, 26]. Figure 3 illustrates temperature dependence of the ratios C_R/u^2 and C_R/σ^2 of Cu, calculated using the present theory. These results show percentages of the correlation effects contributing to the thermodynamic properties of fcc crystals, e.g., to MSD or uncorrelated DWF and to MSRD or correlated DWF, respectively. They are constant at high temperatures, beginning from the Einstein temperature. This indicates that at these high temperatures, the temperature dependence of $\sigma^2(T)$, $u^2(T)$, and $C_R(T)$ of Cu is similar. The result for C_R/u^2, calculated using the present theory, is found to be in reasonable agreement with those calculated using the force constant model (FCM) $C_R/u^2 = 0.415$ [25] and the Debye model (DM) $C_R/u^2 = 0.387$ [26]. Moreover, the ratio C_R/u^2 presented in Fig. 3 is greater than C_R/σ^2. This shows that the correlation effect compared to MSD or uncorrelated DWF is larger than the one compared to MSRD or correlated DWF.

4. Conclusions

In this work, a method has been derived, enabling the calculation and analysis of the temperature-dependent correlated DWF $\sigma^2(T)$, uncorrelated $u^2(T)$, and the correlation function $C_R(T)$ in atomic vibrations of materials based on CEM and UCEM, including many-body effects.

The many-body effects shown in the derived analytical expressions of the correlated DWF $\sigma^2(T)$, uncorrelated DWF $u^2(T)$, and correlation function $C_R(T)$ have been achieved by using CEM and UCEM, i.e., models including the contributions of all nearest neighbors of the absorber and backscatter atoms (for CEM) and a single atom (for UCEM), as well as formulate their effective potentials in the useful form of one-dimensional model.

The present theory has significantly simplified a complicated many-body system task into a one-dimensional model, as well as provided a method for determining the uncorrelated DWF or MSD and correlation function that is simpler than those using X-ray absorption or neutron diffraction and other theories.

The correlation effect has been described based on only the effective local force constants of the harmonic effective potentials obtained by the CAV model used in CEM and the SAV model used in UCEM, which clearly proves that it is a harmonic effect.

The difference between the correlated DWF determined by CEM and the uncorrelated DWF determined by UCEM is considered to be the source causing the correlation effect. It has the same dimension as DWF, and is temperature and crystal types dependent. The larger this difference is, the stronger correlation effect it generates.

The reasons for the difference in the thermodynamic properties of crystals described by the correlated DWF $\sigma^2(T)$ for the CAV model used in CEM and by the uncorrelated DWF u^2(T) for the SAV model used in UCEM are attributed to the difference in their effective local force constants caused by the difference in the number and the mass of vibrating atoms between these models, where for the SAV model they are double compared to those for the CAV model.

The ratios C_R/u^2 and C_R/σ^2 provide percentages of the correlation effects contributing to the thermodynamic properties of crystals described by the functions $u^2(T)$ and $\sigma^2(T)$, respectively. Their constant values at high temperatures indicate the similarity in temperature dependence of the considered values, e.g., the correlated DWF $\sigma^2(T)$, the uncorrelated DWF $u^2(T)$, and the correlation function $C_R(T)$, at these high temperatures.

The present theory avoids the intensive FLD calculations required by a many-body system task, yet it provides a good agreement of the calculated results of $\sigma^2(T)$, $u^2(T)$, and $C_R(T)$ of Cu with the experimental ones obtained from the MMPs, the measured values for $\sigma^2(T)$, as well as values calculated using FCM and DM for C_R/u^2 of Cu. This illustrates the simplicity, advantages, and efficiency of the present theory in EXAFS data analysis, especially in studying the correlated DWF $\sigma^2(T)$, the uncorrelated DWF u^2(T), and the correlation function C_R(T) in EXAFS theory.

This theory can also be applied to the study of the considered quantities of other fcc crystals that were not considered in this work, and it can also be generalized to research these values of other crystal structures based on the calculation of the CAV and SAV local force constants of these materials.

Acknowledgments

The authors thank J.J. Rehr and P. Fornasini for their useful comments and suggestions.

References

[1] E.D. Crozier, J.J. Rehr, R. Ingalls, in: *X-ray Absorption: Principles, Applications, Techniques of EXAFS, SEXAFS and XANES*, Wiley, New York 1988, Ch. 9, p. 373.

[2] E.A. Stern, P. Livins, Zhe Zhang, *Phys. Rev. B* **43**, 8850 (1991).

[3] L. Tröger, T. Yokoyama, D. Arvanitis, T. Lederer, M. Tischer, K. Baberschke, *Phys. Rev. B* **49**, 888 (1994).

[4] N.V. Hung, R. Frahm, *Physica B* **208–209**, 97 (1995).

[5] N.V. Hung, R. Frahm, H. Kamitsubo, *J. Phys. Soc. Jpn.* **65**, 3571 (1996).

[6] N.V. Hung, *J. Phys. IV France* **7**, C2-279 (1997).

[7] J.M. Tranquada, R. Ingalls, *Phys. Rev. B* **28**, 3520 (1983).

[8] A.I. Frenkel, J.J. Rehr, *Phys. Rev. B* **48**, 585 (1993).

[9] T. Yokoyama, *Phys. Rev. B* **57**, 3423 (1998).

[10] T. Miyanaga, T. Fujikawa, *J. Phys. Soc. Jpn.* **63**, 1036 (1994).

[11] T. Miyanaga, T. Fujikawa, *J. Phys. Soc. Jpn.* **63**, 3683 (1994).

[12] A.V. Poiarkova, J.J. Rehr, *Phys. Rev. B* **59**, 948 (1999).

[13] F.D. Vila, J.J. Rehr, H.H. Rossner, H.J. Krappe, *Phys. Rev. B* **76**, 014301 (2007).

[14] S. a Beccara, G. Dalba, P. Fornasini, R. Grisenti, F. Pederiva, A. Samson, *Phys. Rev. B* **68**, 140301(R) (2003).

[15] N.V. Hung, J.J. Rehr, *Phys. Rev. B* **56**, 43 (1997).

[16] N.V. Hung, N.B. Trung, B. Kirchner, *Phys. B* **405**, 2519 (2010).

[17] N.V. Hung, N.B. Duc, R.R. Frahm, *J. Phys. Soc. Jpn.* **72**, 1254 (2003).

[18] M. Daniel, D.M. Pease, N. Van Hung, J.I. Budnick, *Phys. Rev. B* **69**, 134414 (2004).

[19] N.V. Hung, *J. Phys. Soc. Jpn.* **83**, 024802 (2014).

[20] N.V. Hung, N.B. Duc, D.Q. Vuong, T.S. Tien, N.C. Toan, *Radiat. Phys. Chem.* **80**, 109263 (2020).

[21] N.V. Hung, C.S. Thang, N.C. Toan, H.K. Hieu, *Vacuum* **101**, 63 (2014).

[22] P. Wu, K. Xia, K. Peng et al., *Phys. Rev. B* **103**, 195204 (2021).

[23] N.C. Toan, D.Q. Vuong, N.V. Hung, *Acta Phys. Pol. A* **140**, 27 (2021).

[24] N.C. Toan, N.V. Hung, *Acta Phys. Pol. A* **144**, 38 (2023).

[25] R.M. Niclow, G. Gilat, H.G. Smith, R.J. Raubenheimer, M.K. Wikinson, *Phys. Rev.* **164**, 922 (1967).

[26] G. Beni, P.M. Platzman, *Phys. Rev. B* **14**, 1514 (1976).

[27] I.V. Pirog, T.I. Nedoseikina, A.I. Zarubin, A.T. Shuvaev, *J. Phys. Condens. Matter* **14**, 1825 (2002).

[28] R.B. Greegor, F.W. Lytle, *Phys. Rev. B* **20**, 4908 (1979).

[29] T. Yokoyama, T. Sasukawa, T. Ohta, *Jpn. J. Appl. Phys.* **28**, 1905 (1989).

[30] B.T.M. Willis, A.W. Pryor *Thermal Vibrations in Crystallography*, Cambridge University Press, Cambridge, 1975.

[31] L.A. Girifalco, W.G. Weizer, *Phys. Rev.* **114**, 687 (1959).